

# Alkaline and ultrasonic dissolution of biological materials for trace silicon determination

Robert D. Viveros

Department of Nanoengineering, University of California, San Diego, 4112 Pacific Hall,  
9500 Gilman Drive 0358, La Jolla, California 92093

Alexander Liberman

Materials Science and Engineering Program, University of California, San Diego, 4112 Pacific Hall,  
9500 Gilman Drive 0358, La Jolla, California 92093

William C. Trogler

Department of Chemistry and Biochemistry, University of California, San Diego, 4100C Pacific Hall,  
9500 Gilman Drive 0358, La Jolla, California 92093

Andrew C. Kummel<sup>a)</sup>

Department of Chemistry and Biochemistry, University of California, San Diego, B100E Pacific Hall,  
9500 Gilman Drive 0358, La Jolla, California 92093

(Received 31 December 2014; accepted 18 March 2015; published 1 April 2015)

A simple method for trace elemental determination in biological tissue has been developed. Novel nanomaterials with biomedical applications necessitate the determination of the *in vivo* fate of the materials to understand their toxicological profile. Hollow iron-doped calcined silica nanoshells have been used as a model to demonstrate that potassium hydroxide and bath sonication at 50 °C can extract elements from alkaline-soluble nanomaterials. After alkali digestion, nitric acid is used to adjust the *pH* into a suitable range for analysis using techniques such as inductively coupled plasma optical emission spectrometry which require neutral or acidic analytes. In chicken liver phantoms injected with the nanoshells, 96% of the expected silicon concentration was detected. This value was in good agreement with the 94% detection efficiency of nanoshells dissolved in aqueous solution as a control for potential sample matrix interference. Nanoshell detection was further confirmed in a mouse 24 h after intravenous administration; the measured silica above baseline was 35 times greater or more than the standard deviations of the measurements. This method provides a simple and accurate means to quantify alkaline-soluble nanomaterials in biological tissue.

© 2015 American Vacuum Society. [<http://dx.doi.org/10.1116/1.4916627>]

## I. INTRODUCTION

Nanotechnology has demonstrated great potential in biomedical applications such as drug delivery, *in vivo* imaging, and disease therapeutics.<sup>1–4</sup> To assess the safety of nanomaterials, it is necessary to understand their *in vivo* fate. Analysis of animal model organs for the presence of the nanomaterials helps define their biodistribution and elimination pathways.

Detection of nanomaterials or other target analytes requires effective preparation of the collected biological tissue, and digestion has been extensively investigated to serve this purpose. Tissue has been proven to be digestible in acids, such as nitric acid,<sup>5–7</sup> and in bases such as alkali hydroxides.<sup>8–12</sup> Tissue drying, powdering, homogenization, or other sample pretreatment methods are used in several existing acid- or base-facilitated tissue digestion methods.<sup>5,8,12–14</sup> External techniques, such as heating, sonication, and microwave or autoclave irradiation, have also been used to great effect.<sup>5–8,11,12,14–19</sup> To improve measurement accuracy, several techniques include an internal standard, such as yttrium, which is naturally present in biological specimens in extremely low background concentrations.<sup>6,13–15</sup> Many of

these techniques face limitations, such as sample loss or convolution from tissue matrix effects. It is known that the contents of the sample matrix can adversely influence element detection sensitivity when using techniques such as inductively coupled plasma optical emission spectrometry (ICP-OES) or mass spectrometry (ICP-MS).<sup>20</sup>

Several biodistribution studies of nanoparticles using chemical spectroscopic methods have been reported. The biodistribution of gold nanoparticles of various sizes, geometries, and surface chemistries in rodents has been extensively investigated.<sup>15–17,19,21</sup> The *in vivo* localization of the gold nanoparticles in these experiments has been demonstrated using ICP-MS or graphite furnace atomic absorption spectrometry (GFAAS). Sample preparation was generally performed using acidic mixtures such as aqua regia. Several studies incorporated an internal standard to improve measurement accuracy. Copper nanoparticle biodistribution has also been reported in nematodes using HNO<sub>3</sub>/H<sub>2</sub>O<sub>2</sub> for digestion and ICP-MS as one method of analysis.<sup>22</sup> Hirst *et al.* demonstrated the biodistribution of ceria nanoparticles in mice using concentrated HNO<sub>3</sub> with microwave irradiation for digestion and ICP-MS for cerium determination.<sup>18</sup> The biodistribution of silver nanocrystals in rats using ICP-MS after organ digestion was also reported.<sup>23</sup> Chertok *et al.* used both ICP-OES and electron spin resonance spectroscopy for measuring the

<sup>a)</sup>Electronic mail: akummel@ucsd.edu

biodistribution of iron-oxide nanoparticles in rats.<sup>14</sup> The collected organs were homogenized, digested in concentrated HCl, diluted with H<sub>2</sub>O, and spiked with yttrium as an internal standard for ICP-OES analysis.

Alternatively, solid sampling methods using high-resolution continuum source graphite furnace atomic absorption spectrometry (HR CS GFAAS) have demonstrated high sensitivity for analyte concentration determination in various biological specimens. Resano *et al.* performed biodistribution studies of gold nanoparticles in mice by drying, manually grounding, adding a chemical modifier for analyte stability, and analyzing the organs for gold concentration.<sup>24</sup> Similarly, silver quantification in small invertebrates was performed by exposing the specimens to the AgNO<sub>3</sub> or silver nanoparticles, washing and drying the specimens, adding a chemical modifier, and analyzing the specimens using HR CS GFAAS.<sup>25</sup>

The biodistributions of silicon and silica nanoparticles have also been determined using chemical spectroscopic methods; some techniques used acids such as HF which pose safety concerns. Park *et al.* demonstrated that biodegradable luminescent porous silicon nanoparticles can be detected in the organs of mice after intravenous administration using ICP-OES.<sup>26</sup> The organs were digested in a solution containing HNO<sub>3</sub>, H<sub>2</sub>O<sub>2</sub>, and HF over the course of 2 days, and H<sub>3</sub>BO<sub>3</sub> was added to the samples in addition to 2% HNO<sub>3</sub> for dilution before analysis. ICP-MS has been utilized to demonstrate enhanced tumor uptake of fluorescent mesoporous silica nanoparticles with folic acid conjugation when compared to unmodified nanoparticles in mice with xenograft tumors.<sup>27</sup> The collected organs and tumor tissue were digested in a 1:1:1 solution of H<sub>2</sub>O, HF, and HNO<sub>3</sub> with heating for analysis. Alkaline digestion has been previously used for silicon determination in tumor-bearing mice, which received intravenous administration of silicon or silica particles.<sup>13</sup> The collected organs and tumors were homogenized in ethanol and 1 N NaOH and were digested over the course of 48 h. The samples were centrifuged, and the supernatants were diluted with H<sub>2</sub>O and spiked with yttrium before ICP-OES analysis. Similarly, the biodistribution of silica coated NaYF<sub>4</sub> nanocrystals in rats was determined using ICP-OES.<sup>28</sup> The organs were digested in a mixture of potassium hydroxide (KOH) and Tween-80 overnight at 37 °C, and the samples were filtered before yttrium determination. To our knowledge, none of these techniques neutralized the alkaline solutions nor did they quantify the percent silica recovery of the sample preparation technique.

It has been shown that accurate element determination of digested biological samples can be achieved using spectroscopic techniques. Morais *et al.* analyzed gold-spiked rat organs after acid digestion using GFAAS.<sup>19</sup> Gold recovery in the various organs ranged from 85.8% to 109%. Analyte recovery of several elements in ultrasonic digested lichen and muscle tissue samples was shown to increase with increasing acid solution concentration up to 1% by volume.<sup>6</sup> Samples digested in 1% HNO<sub>3</sub>, 1% HCl, or 1% HNO<sub>3</sub> with 1% HCl consistently gave 90%–100% analyte recovery for most target elements using ICP-OES and ICP-MS. Studies performed by Hauptkorn *et al.* demonstrated 90.4%

detection of the theoretical silicon concentration of silicon-spiked, tetramethylammonium hydroxide-digested pork liver samples using ICP-OES.<sup>10</sup>

While HF is known to be capable of dissolving silica, it poses health and safety risks which makes it an unattractive dissolution agent.<sup>29</sup> Alkali hydroxides are alternatively known to dissolve both silica gel<sup>30</sup> and calcined silica.<sup>31</sup> For example, hollow TiO<sub>2</sub> nanoshells have previously been synthesized by NaOH etching of a calcined silica coated TiO<sub>2</sub> layer on a silica template. Because KOH poses lesser safety risks, it was selected as an alternative over HF. With this method, tissue can be minimally processed under basic conditions to isolate materials that are alkaline soluble, and the solution can be returned to a pH compatible with analysis equipment using acid neutralization. This method additionally shows minimal to no analyte loss. The method employs simultaneous digestion of tissue and calcined silica nanomaterials using aqueous KOH and bath sonication followed by acid neutralization. After KOH dissolution, samples were neutralized using dilute HNO<sub>3</sub> for the safety of the analytical instrumentation which is susceptible to destruction from basic or strongly acidic samples. In addition, an internal yttrium calibration standard was incorporated, resulting in improved accuracy.

The present method is focused on detection of calcined silica nanoshells in tissue. These nanoshells have previously been described and have found applications as ultrasound contrast agents and high intensity focused ultrasound sensitizing agents.<sup>32,33</sup> The utility of the method may be extended to other alkaline-soluble nanomaterials, biomaterials, and pharmaceuticals. The method described here was developed to simultaneously dissolve tissue samples and silica nanoshells and to process the solutions to a suitable pH range for ICP-OES analysis.

## II. EXPERIMENTAL DETAILS

### A. Materials

Tetramethyl orthosilicate was purchased from Sigma-Aldrich (St. Louis, MO). Iron(III) ethoxide was obtained from Gelest Inc. (Moorisville, PA), and 500 nm polystyrene and polyamine-functionalized polystyrene templates were provided by Polysciences (Warrington, PA). A Millipore SuperQ Plus Water Purification System (Billerica, MA) was used to attain purified MilliQ water. KOH pellets were purchased from Fischer-Scientific (Pittsburg, PA). Aqueous KOH of 500 mM was obtained by dissolving the KOH pellets in Milli-Q water. Nitric acid (HNO<sub>3</sub>) was provided by EMD Millipore (Billerica, MA) at 67%–70% purity. One percent HNO<sub>3</sub> was prepared by diluting the stock HNO<sub>3</sub> using MilliQ water. The multielement standard solution for silicon calibration was provided by SPEX CertiPrep (Metuchen, NJ). The yttrium standard solution for internal calibration was purchased from Agilent Technologies (Santa Clara, CA). Chicken liver and breast phantoms were obtained from a local grocery store. ICP-OES analysis was performed using the Perkin Elmer (Waltham, MA) Optima 3000 DV. Silicon measurements were taken at 251.611 nm, and yttrium measurements were taken at 371.029 nm.

## B. Animals

Six week old female Swiss white mice were provided by Charles River Laboratories, weighing between 20 and 25 g each. Mice were fed commercial pelleted diet provided and Harlan Tekland and kept at 22 °C in University of California, San Diego (UCSD) approved animal housing with a 12 h light/dark cycle. All animal care and procedures were approved the UCSD Institutional Animal Care and Use Committee.

## C. Synthesis of iron-doped silica nanoshells

The synthesis of hollow iron-doped silica nanoshells has been previously reported (formulation 1). Briefly, a 20 mg/ml solution of ethanolic iron ethoxide was sonicated for 1 h, and 10  $\mu$ l of the iron ethoxide and 2.7  $\mu$ l of tetramethyl orthosilicate were mixed and sonicated for 10 min. Fifty microliters of polyamine-functionalized polystyrene bead solution was added to 1 ml of absolute ethanol. Iron ethoxide and tetramethyl orthosilicate mixture of 12.7  $\mu$ l was added, and the resulting solution was vortex mixed for 5 h. The solution was centrifuged for 10 min at 3000 rpm, the supernatant was removed, and the remaining sample was washed twice with ethanol. The sample was calcined for 18 h at 550 °C. The yield per batch is approximately 0.6–0.8 mg.

Additionally, a modified synthetic procedure was used to synthesize the nanoshells for the ICP-OES analysis of nanoshell-injected tissue phantoms (formulation 2). Polystyrene bead solution of 50  $\mu$ l was added to 1 ml of 95% ethanol. A proprietary mixture was added, and the resulting mixture was vortexed at 3000 rpm for 1 h. Ten microliters of a 20 mg/ml solution of iron ethoxide and 2.7  $\mu$ l of tetramethyl orthosilicate were added, and the mixtures were vortex mixed for 5 h. The solution was centrifuged for 10 min at 3000 rpm, the supernatant was removed, and the remaining sample was washed twice with ethanol. The sample was then calcined for 18 h at 550 °C. The resulting hollow iron-doped silica nanoshells were weighed and stored dry until use. These nanoshells were used as a model for alkaline-soluble nanomaterials. The nanomaterial yield per batch is approximately 0.3–0.4 mg.

## D. Ultrasound-assisted dissolution of nanoshells

Nanoshell dissolution was demonstrated using both nanoshell formulations. One milligram of each formulation was incubated in 1 ml of aqueous 500 mM KOH. These samples were sonicated over the course of 24 h, and scanning electron microscopy (SEM) images were taken after 1 and 24 h of base treatment.

## E. ICP-OES analysis of standard solutions in tissue phantoms

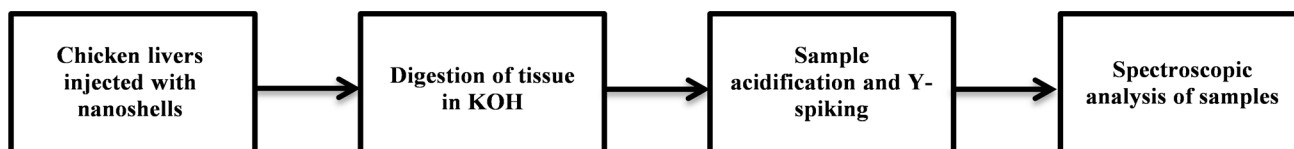
Experiments were performed in tissue phantoms to investigate measurement accuracy. Digested and acidified chicken liver tissue phantoms were spiked with a silicon standard solution to result in a range of final silicon concentrations. Control samples were prepared by diluting standard solutions in 1% HNO<sub>3</sub> to match the expected silicon concentrations in the tissue phantom counterparts. The 1 g tissue samples were digested in 7 ml of 500 mM KOH, acidified using 2.5 ml of 1% HNO<sub>3</sub> added to 0.5 ml of the sample solution, diluted by withdrawing 1 ml of the supernatant after centrifugation at 3000 rpm for 15 min and making the volume up to 5 ml using 1% HNO<sub>3</sub>, and centrifuged before analysis to isolate potential reprecipitated particulates.

## F. ICP-OES analysis of nanoshells in tissue phantoms

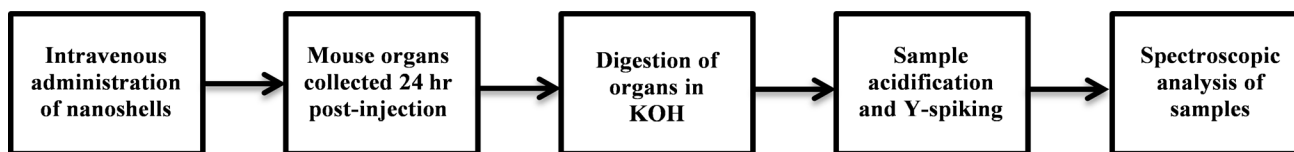
The process for nanoshell detection in biological tissue is outlined in Scheme 1. One gram chicken liver tissue phantoms were injected with 100  $\mu$ l of aqueous nanoshell solutions (formulation 2) of initial concentrations at 0.25, 1, 4, and 8 mg/ml. The samples were immersed in 7 ml of 500 mM KOH and bath sonicated for 48 h. Control samples were prepared by directly adding the 100  $\mu$ l of nanoshell solutions to KOH and processed with the same preparation method as the tissue samples. The samples were centrifuged for 15 min at 3000 rpm to remove any potential remaining insoluble particulates. The fraction of precipitate in these samples was less than 5%. Supernatants of the digested samples (0.5 ml) were acidified with 2.5 ml of 1% HNO<sub>3</sub> and centrifuged for 15 min at 3000 rpm. These samples were centrifuged for 15 min at 3000 rpm to isolate potential reprecipitated tissue. A 300  $\mu$ g/l yttrium standard solution (0.5 ml) was added to each 2.5 ml aliquot of a supernatant sample. The resulting solutions were diluted in 1% HNO<sub>3</sub> by a factor of five to fall into a suitable concentration range for detection and were briefly centrifuged immediately before ICP-OES analysis. Four samples were prepared for each expected concentration for both the tissue samples and the aqueous controls.

## G. ICP-OES analysis of nanoshells in murine organs

Two healthy Swiss mice were used to assess this method to detect iron-doped silica nanoshells in mouse organs. Scheme 2 outlines the process for nanoshell quantification in mouse organs. One mouse was injected with 100  $\mu$ l of a 4 mg/ml aqueous nanoshell solution (formulation 1). The second mouse received no injection. The mice were sacrificed 24 h after the first mouse received the nanoshell injection, and the organs



SCHEME 1. Flow diagram of procedure for nanoshell detection in tissue phantoms. The potential for Fe-doped silica nanoshell detection in biological tissue using the described method was determined by injecting the nanoshells into 1 g chicken livers, processing the phantoms for analysis, and analyzing the samples using ICP-OES for trace Si and Y determination.



SCHEME 2. Flow diagram of procedure for nanoshell detection in mouse organs. The *in vivo* fate of Fe-doped silica nanoshells was determined by intravenously injecting the nanoshells into mice, processing the organs for analysis 24 h postinjection, and analyzing the samples using ICP-OES for trace Si and Y determination.

were collected. To analyze the organs for silicon content, the organs were incubated in 7 ml of aqueous 500 mM KOH and bath sonicated for 48 h. Each digested sample (0.5 ml) was drawn out and acidified using 2.5 ml of 1% HNO<sub>3</sub>. The samples were centrifuged for 15 min at 3000 rpm, and 0.5 ml of a 300  $\mu$ g/l yttrium standard solution was added to each 2.5 ml aliquot of a supernatant sample. The samples were briefly centrifuged immediately before ICP-OES analysis.

### III. RESULTS AND DISCUSSION

#### A. Ultrasound-assisted dissolution of nanoshells

To develop a high efficiency method for extracting the silicon from the nanoshells, KOH was investigated for dissolving the silica of the nanoshells. As shown in Fig. 1, all formulations demonstrated complete nanoshell dissolution within 1 h of KOH incubation with bath sonication. The presence of silicon in the dissolved samples was confirmed by energy dispersive x-ray spectroscopy (data not shown). Dehydrated silica salts were observed by SEM imaging after the solvent was evaporated and constituted some of the observed residual material. This indicates that KOH is capable of dissolving the nanoshells to extract the silicon in a soluble form for analysis.

#### B. ICP-OES analysis of standard solutions in tissue phantoms

Low baseline silicon levels of biological tissue and minimal detection interference from the sample matrix were confirmed by digesting 1 g of chicken liver with 500 mM KOH and bath sonication and acidifying the samples using 1% HNO<sub>3</sub>. A multielement standard solution containing a known silicon concentration was added to the samples to create a known silicon concentration. Control samples were prepared by diluting the standard solution in 1% HNO<sub>3</sub> to match the concentrations of the tissue samples. As shown in Fig. 2, measurements of detected silicon concentration against expected silicon concentration demonstrate that there was little discrepancy between the control (blue diamond) and tissue (red square) samples. These results show that the presence of tissue had minimal impact on silicon detection which validates the reliability of silicon measurements using this processing method.

#### C. ICP-OES analysis of nanoshells in tissue phantoms

To determine the accuracy of this method for trace silicon determination of biological tissue containing silica nanoshells, 1 g chicken liver samples were injected with 100  $\mu$ l of a 0.25, 1, 4, or 8 mg/ml aqueous nanoshell solutions. The

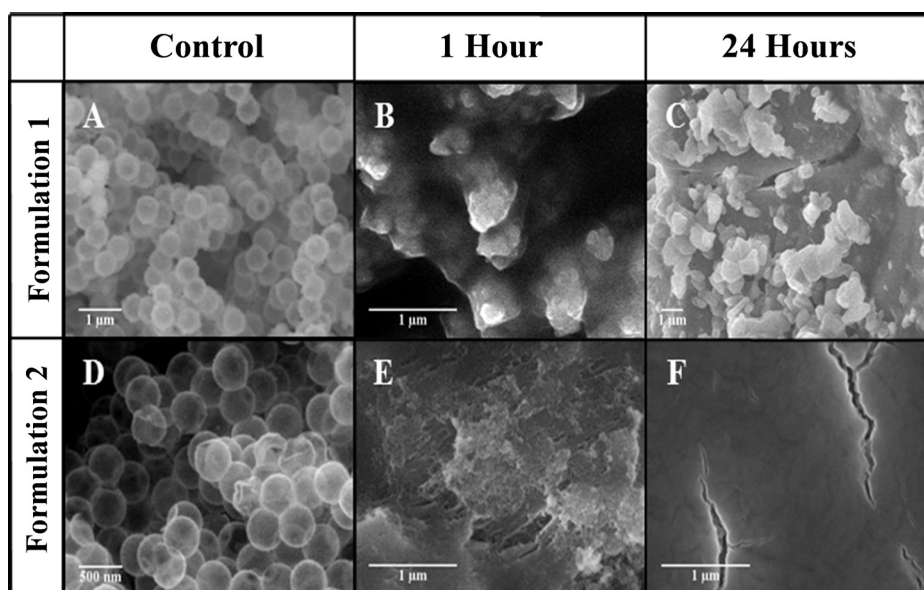


FIG. 1. Nanoshells were dissolved in KOH to demonstrate that silicon is extractable at 50 °C for elemental determination. [(a)–(c)] SEM images are shown of formulation 1 nanoshells and of formulation 1 nanoshells dissolved in 500 mM KOH for 1 and 24 h. [(d)–(f)] SEM images are shown of formulation 2 nanoshells and of formulation 2 nanoshells dissolved in 500 mM KOH for 1 and 24 h.

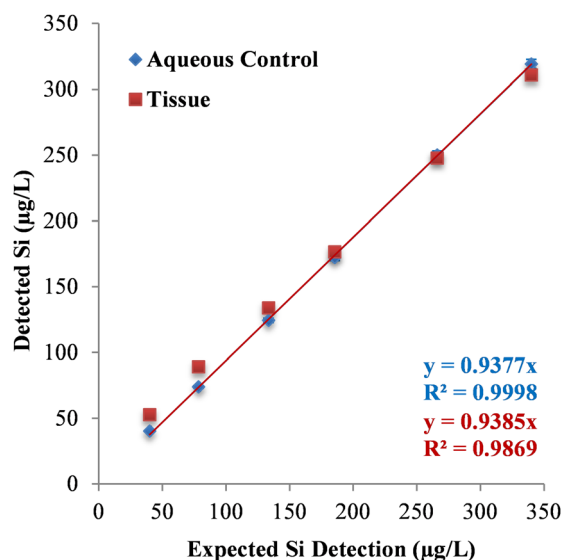


FIG. 2. (Color online) Si determination in Si standard-injected tissue. Chicken livers were digested and acidified, and known volumes of a Si standard solution were added to the samples to generate known Si concentrations. Control measurements were taken by diluting the Si standard with  $\text{HNO}_3$  to match the expected Si concentrations in the tissue sample set. The digested chicken liver was observed to have little influence on detected Si. Standard deviations are shown for four replicates of each sample.

samples were digested for 48 h in 500 mM KOH and centrifuged for 15 min at 3000 rpm. Supernatants (0.5 ml) were drawn out and added to 2.5 ml of 1%  $\text{HNO}_3$  for acidification. Potential reprecipitated tissue particulates were isolated by centrifugation, and 0.5 ml of a 300  $\mu\text{g/l}$  yttrium standard solution was added to 2.5 ml of the supernatants. Control experiments were performed by dissolving the nanoshells directly in the corresponding volume of aqueous KOH and following the same procedure. The expected silicon detection concentration was estimated based on elemental composition of the nanoshells obtained from energy dispersive x-ray spectroscopy. Figure 3 illustrates a detection of 82% and 90% of the expected concentration of silicon in the aqueous controls (blue diamond) and tissue samples (red square), respectively. The small discrepancies between the expected and detection concentration of silicon may arise from measurement drift in the instrument and from estimation errors regarding the ratio of element composition of the nanoshells. The elemental weight composition used for calculations was based on dehydrated ( $\text{SiO}_2$ ) nanoshells, whereas the nanoshells from the study likely contained some adsorbed water from atmospheric exposure before and during weighing, accounting for the reduced value of silicon detected.

To eliminate potential measurement drift in the instrument and sample matrix effects, an yttrium internal standard was used as a correction method. As shown in Fig. 4, yttrium measurements were consistent for all the samples despite the very low concentrations being measured. Yttrium detection was expected at 10  $\mu\text{g/l}$ , so the silicon measurements were adjusted based on the ratio of the detected yttrium to expected yttrium detection. The greater yttrium detection in the tissue samples was consistently within 1  $\mu\text{g/l}$  of the

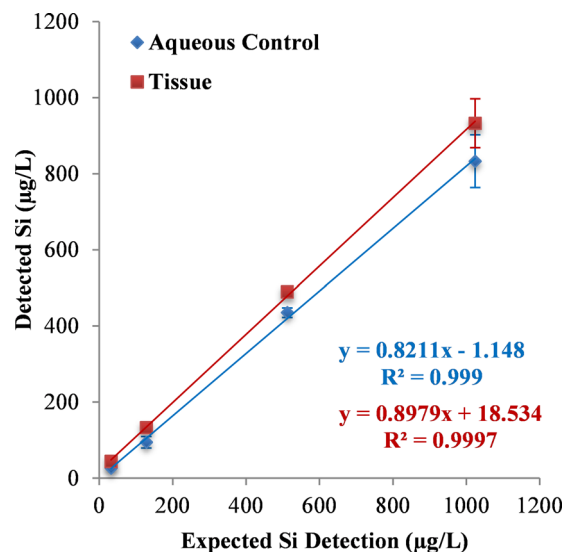


FIG. 3. (Color online) Si determination in iron-doped silica nanoshell-injected tissue. Chicken livers were injected with 100  $\mu\text{l}$  of nanoshells, digested in KOH, and acidified in  $\text{HNO}_3$ . Control measurements were taken by directly adding the nanoshells to KOH and following the same procedure afterwards. The digested tissue samples were in agreement with the controls, and the majority of the expected Si concentration was detected. Standard deviations are shown for four samples at each concentration per set.

control; therefore, the sample matrix interference was observed to be minimal but quantifiable.

Silicon detection was corrected to 94% and 96% of the expected silicon concentration in the control (blue diamond) and tissue phantom (red square) sets, resulting in close agreement with the expected values based on estimation (Fig. 5). After the yttrium based correction, the two silicon recoveries are nearly identical, validating the results from standard solution experiments. These results indicate that silicon determination can be reliably performed on silica

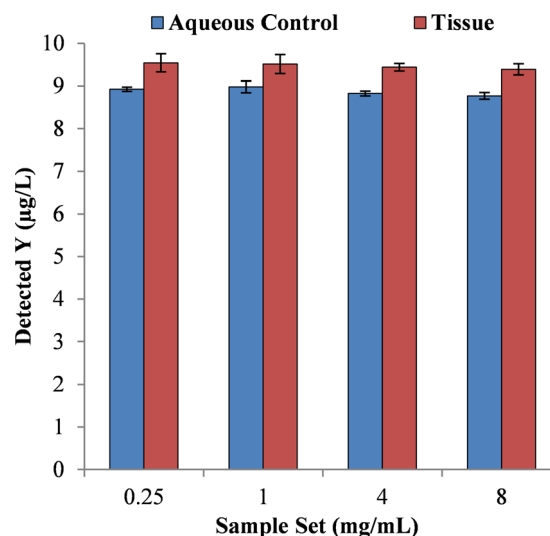


FIG. 4. (Color online) Y determination in tissue phantoms and aqueous controls. The aqueous controls and tissue samples were spiked with an yttrium standard solution for a final concentration of 10  $\mu\text{g/l}$ . Detection was consistent among each set, and the tissue samples were within 1  $\mu\text{g/l}$  of the aqueous controls. Standard deviations are shown for four samples at each concentration per set.

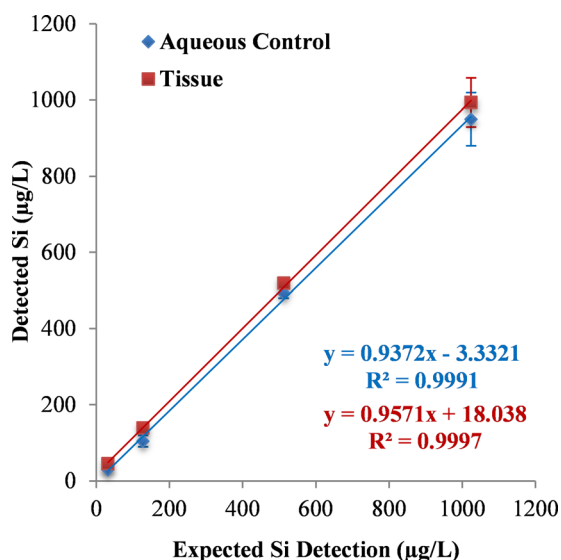


Fig. 5. (Color online) Si determination after Y correction. The results from the Si determination in nanoshell-injected tissue samples and aqueous controls were reprocessed using the ratio of detected to expected detection of Y detection to scale silicon detection. Approximately 94% and 96% of the expected Si concentration was detected in the control and tissue samples. Standard deviations are shown for four samples at each concentration per set.

nanoshell-bearing biological tissue with this method when applying an internal standard to correct for instrument error and drift.

#### D. ICP-OES analysis of nanoshells in murine organs

A healthy Swiss white mouse was injected intravenously in the tail vein with 100  $\mu$ l of an aqueous 4 mg/ml nanoshell solution. The mouse was sacrificed 24 h after injection, and the organs were collected, processed, and analyzed. Four replicates of each sample were analyzed for error analysis. Yttrium detection was consistent across all analyzed organs,

and silicon in the nanoshell-injected mouse was detected only in the lung and liver of the mouse (Fig. 6). The raw silicon concentrations corresponded to approximately 9.6% and 7.0% of the initial injected dose, respectively. These levels were appreciably above baseline control levels and 35 times greater or more than the standard deviations of the measurements, indicating that the presence of the nanoshells was significant.

#### IV. SUMMARY AND CONCLUSIONS

A method has been presented which allows for quantitative high recovery trace elemental determination of alkaline-soluble nanomaterials in biological tissue. The present method avoids HF, heating, and microwave processing and provides full neutralization to insure the samples are compatible with analytical equipment. The calibrated silicon measurements obtained from the method presented here provide target analyte recovery comparable to other existing spectroscopic sample preparation methods. This facile tissue processing method provides minimal sample loss, allows for multiple analyses due to a large final sample volume, and offers a higher safety margin than potential alternative techniques. This work provides a general procedure for the accurate determination of the *in vivo* fate of silica and other alkaline-soluble nanomaterials with biomedical applications. Analysis of tissue phantoms injected with iron-doped silica nanoshells demonstrated that raw silicon determination of the processed samples showed agreement within 8% of the aqueous controls. Implementing an internal standard that is not naturally present in biological specimens in appreciable quantities offers a beneficial tool to correct and assess instrumental and sample preparation reproducibility. The internal standard calibrated results improve the agreement between the tissue samples and the aqueous controls to within 2%. ICP-OES analysis of an iron-doped silica nanoshell-injected mouse demonstrated *in vivo* measurement of the nanoshells; the observed values of silica above baseline were 35 times

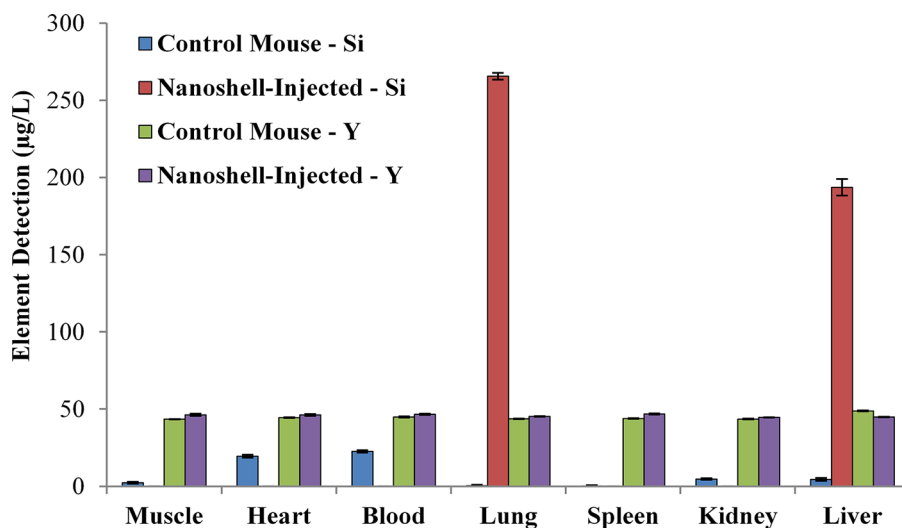


Fig. 6. (Color online) Determination of Si and Y in mouse organs. A mouse was injected with nanoshells, and the organs were collected 24 h later. A control mouse was sacrificed which received no injection. Both sample sets were spiked with Y. Si detection from the nanoshells was observed in the lung and liver of the nanoshell-injected mouse at 9.6% and 7.0% of the initial injected dose. Standard deviations are shown for four replicates of each sample; the majority of these values are approximately 1  $\mu$ g/l or less.

greater than the standard deviation of the measurement. This biological sample preparation method should be generally useful for elemental determination of alkaline-soluble nanomaterials and is directly applicable to trace element detection spectroscopic techniques such as ICP-OES.

## ACKNOWLEDGMENTS

This study has been funded by the 1R21CA151140-01A2 and the NIH IMAT 1R33CA177449-01A1. Individual student funding was provided by NIH Ruth L. Kirschstein National Research Service Award F31 Fellowship (NIH Grant No. 1F31CA174276) and the NIH—Cross Training Translation Cancer Researchers in Nanotechnology (CRIN) Grant No. (NIH 3 R25 CA 153915). The content is solely the responsibility of the authors and does not necessarily represent the official views of the National Institutes of Health.

- <sup>1</sup>O. C. Farokhzad and R. Langer, *ACS Nano* **3**, 16 (2009).
- <sup>2</sup>N. Portney and M. Ozkan, *Anal. Bioanal. Chem.* **384**, 620 (2006).
- <sup>3</sup>A. Liberman, N. Mendez, W. C. Trogler, and A. C. Kummel, *Surf. Sci. Rep.* **69**, 132 (2014).
- <sup>4</sup>X. Gao, Y. Cui, R. M. Levenson, L. W. K. Chung, and S. Nie, *Nat. Biotechnol.* **22**, 969 (2004).
- <sup>5</sup>R. S. Yang, L. W. Chang, J.-P. Wu, M.-H. Tsai, H.-J. Wang, Y.-C. Kuo, T.-K. Yeh, C. S. Yang, and P. Lin, *Environ. Health Perspect.* **115**, 1339 (2007).
- <sup>6</sup>M. Krishna and J. Arunachalam, *Anal. Chim. Acta* **522**, 179 (2004).
- <sup>7</sup>E. De Oliveira, J. McLaren, and S. Berman, *Anal. Chem.* **55**, 2047 (1983).
- <sup>8</sup>F. Y. Leung and P. Edmond, *Clin. Biochem.* **30**, 399 (1997).
- <sup>9</sup>S. Lo, J. Russell, and A. Taylor, *J. Appl. Physiol.* **28**, 234 (1970), available at <http://jap.physiology.org/content/28/2/234>.
- <sup>10</sup>S. Hauptkom, J. Pavel, and H. Seltner, *Fresenius J. Anal. Chem.* **370**, 246 (2001).
- <sup>11</sup>J. P. Ebel, *Pharm. Res.* **7**, 848 (1990).
- <sup>12</sup>E. King, B. Stacy, P. Holt, D. M. Yates, and D. Pickles, *Analyst* **80**, 441 (1955).
- <sup>13</sup>P. Decuzzi, B. Godin, T. Tanaka, S.-Y. Lee, C. Chiappini, X. Liu, and M. Ferrari, *J. Controlled Release* **141**, 320 (2010).
- <sup>14</sup>B. Chertok, A. J. Cole, A. E. David, and V. C. Yang, *Mol. Pharmaceutics* **7**, 375 (2009).
- <sup>15</sup>Arnida, M. M. Janát-Amsbury, A. Ray, C. M. Peterson, and H. Ghandehari, *Eur. J. Pharm. Biopharm.* **77**, 417 (2011).
- <sup>16</sup>W. H. De Jong, W. I. Hagens, P. Krystek, M. C. Burger, A. J. A. M. Sips, and R. E. Geertsma, *Biomaterials* **29**, 1912 (2008).
- <sup>17</sup>X.-L. Huang, B. Zhang, L. Ren, S.-F. Ye, L.-P. Sun, Q.-Q. Zhang, M.-C. Tan, and G.-M. Chow, *J. Mater. Sci.: Mater. Med.* **19**, 2581 (2008).
- <sup>18</sup>S. M. Hirst, A. Karakoti, S. Singh, W. Self, R. Tyler, S. Seal, and C. M. Reilly, *Environ. Toxicol.* **28**, 107 (2013).
- <sup>19</sup>T. Morais *et al.*, *Eur. J. Pharm. Biopharm.* **80**, 185 (2012).
- <sup>20</sup>J. W. Olesik, *Anal. Chem.* **68**, 469A (1996).
- <sup>21</sup>C. Lasagna-Reeves *et al.*, *Biochem. Biophys. Res. Commun.* **393**, 649 (2010).
- <sup>22</sup>Y. Gao *et al.*, *J. Anal. At. Spectrom.* **23**, 1121 (2008).
- <sup>23</sup>L. Garza-Ocanas, D. A. Ferrer, J. Burt, L. A. Diaz-Torres, M. Ramirez Cabrera, V. T. Rodriguez, R. Lujan Rangel, D. Romanovicz, and M. Jose-Yacamán, *Metallomics* **2**, 204 (2010).
- <sup>24</sup>M. Resano, E. Mozas, C. Crespo, J. Briceño, J. del Campo Menoyo, and M. Belarra, *J. Anal. At. Spectrom.* **25**, 1864 (2010).
- <sup>25</sup>M. Resano, A. C. Lapeña, and M. A. Belarra, *Anal. Methods* **5**, 1130 (2013).
- <sup>26</sup>J.-H. Park, L. Gu, G. von Maltzahn, E. Ruoslahti, S. N. Bhatia, and M. J. Sailor, *Nat. Mater.* **8**, 331 (2009).
- <sup>27</sup>J. Lu, M. Liang, Z. Li, J. I. Zink, and F. Tamanoi, *Small* **6**, 1794 (2010).
- <sup>28</sup>R. Abdul Jalil and Y. Zhang, *Biomaterials* **29**, 4122 (2008).
- <sup>29</sup>J. Lee, S. Han, and T. Hyeon, *J. Mater. Chem.* **14**, 478 (2004).
- <sup>30</sup>P. Wijnjen, T. Beelen, J. De Haan, C. Rummens, L. Van de Ven, and R. Van Santen, *J. Non-Cryst. Solids* **109**, 85 (1989).
- <sup>31</sup>J. B. Joo, Q. Zhang, I. Lee, M. Dahl, F. Zaera, and Y. Yin, *Adv. Funct. Mater.* **22**, 166 (2012).
- <sup>32</sup>A. Liberman *et al.*, *ACS Nano* **7**, 6367 (2013).
- <sup>33</sup>A. Liberman *et al.*, *J. Surg. Res.* **190**, 391 (2014).